Correlation of Defect-Related Optoelectronic Properties in Zn5(OH)6(CO3)2/ZnO Nanostructures with Their Quasi-Fractal Dimensionality

Hindawi Publishing Corporation
Journal of Nanomaterials
Volume 2015, Article ID 237985, 6 pages
http://dx.doi.org/10.1155/2015/237985

Research Article

Correlation of Defect-Related Optoelectronic Properties in $Zn_5(OH)_6(CO_3)_2$/ZnO Nanostructures with Their Quasi-Fractal Dimensionality

J. Antonio Paramo,[1] Yuri M. Strzhemechny,[1] Tamio Endo,[2] and Zorica Crnjak Orel[3]

[1]*Department of Physics and Astronomy, Texas Christian University, TCU Box 298840, Fort Worth, TX 76129, USA*
[2]*Department of Electrical and Electronic Engineering, Faculty of Engineering, Mie University, 1577 Kurimamachiya, Tsu, Mie 514-8507, Japan*
[3]*National Institute of Chemistry, Hajdrihova 19, 1000 Ljubljana, Slovenia*

Correspondence should be addressed to Yuri M. Strzhemechny; y.strzhemechny@tcu.edu
and Zorica Crnjak Orel; zorica.crnjak.orel@ki.si

Received 7 December 2014; Revised 11 February 2015; Accepted 19 February 2015

Academic Editor: Ion Tiginyanu

Hydrozincite ($Zn_5(OH)_6(CO_3)_2$) is, among others, a popular precursor used to synthesize nanoscale ZnO with complex morphologies. For many existing and potential applications utilizing nanostructures, performance is determined by the surface and subsurface properties. Current understanding of the relationship between the morphology and the defect properties of nanocrystalline ZnO and hydrozincite systems is still incomplete. Specifically, for the latter nanomaterial the structure-property correlations are largely unreported in the literature despite the extensive use of hydrozincite in the synthesis applications. In our work, we addressed this issue by studying precipitated nanostructures of $Zn_5(OH)_6(CO_3)_2$ with varying quasi-fractal dimensionalities containing relatively small amounts of a ZnO phase. Crystal morphology of the samples was accurately controlled by the growth time. We observed a strong correlation between the morphology of the samples and their optoelectronic properties. Our results indicate that a substantial increase of the free surface in the nanocrystal samples generates higher relative concentration of defects, consistent with the model of defect-rich surface and subsurface layers.

1. Introduction

Zinc oxide is a material with a unique combination of valuable traits: it demonstrates remarkable optical and electrical properties as well as outstanding chemical and environmental stability. ZnO has found extensive use in electronics, sensors, photocatalysis, acoustoelectrical devices, and solar cells. It also shows great potential for spintronic and high-performance optoelectronic applications. Studies of physical and chemical properties of ZnO represent a thriving field with a broad domain of topics [1]. ZnO nanostructures have developed into a significant, diverse, and continuously growing field [2]. Remarkably, nanoscale ZnO structures are offering numerous applications that do not require resolving the challenge of p-type conductivity. Nanosize ZnO could be employed in such systems as dye-sensitized and hybrid solar cells [3–6], nanotransducers [7], random lasers [8], and sensors [9]. This diversity of the range of applications reveals a great potential of nanocrystalline ZnO.

The scope of the reported methods to fabricate ZnO nanostructures is truly remarkable and grows by the day. One of these many methods is a procedure based on converting precursor hydrozincite ($Zn_5(OH)_6(CO_3)_2$) nanostructures into ZnO nanocrystals [10–17]. In particular, this technique was shown to be effective for producing nanoporous nanoscale ZnO useful in potential solar cells [3], as well as photocatalytic and gas sensing applications [15, 16, 18, 19]. By itself, hydrozincite, a naturally occurring basic zinc carbonate, has been researched, mostly in geology-related studies, as well as a catalyst component [20, 21]. Nanoscale

forms of hydrozincite have been known and studied not only as precursors for generating a nanoscale ZnO, but also as, for example, a product of naturally occurring biologically controlled mineralization [22]. Although optical properties of hydrozincite have been investigated by many researchers, the nature of its visible luminescence is still under debate. For example, the characteristic blue luminescence is often attributed to impurities (such as Pb), although this assignment is not certain [23]. Most importantly, the optoelectronic properties of the nanoscale hydrozincite are largely unknown despite the extensive use of this nanomaterial in the synthesis applications. On the other hand, in the literature the studies of the structure-property correlation for nanoscale ZnO synthesized from $Zn_5(OH)_6(CO_3)_2$ were reported (e.g., [24–26]), addressing, in particular, the effects of thermal processing on the properties of resulting nanostructures. Thus, in our view, it is important to know whether the structure-property relationships for the final product are determined by similar relationships for the precursor.

Generally, one of the most important features of a nanostructure affecting its properties is the high surface-to-volume ratio. Because of that, in nanostructures one deals with surface enhanced phenomena, whereas the surface states are likely to influence key performance parameters. It is understood that, in the process of termination and reconstruction, the surface can develop elevated concentration of defects, which may not be necessarily confined within the immediate vicinity of the surface but could also permeate inward driven by diffusion, stress, cation/anion imbalance, and so forth. It is quite natural to assume that such defective layer, with distinct stoichiometric, optoelectronic, and structural characteristics, is a generic feature weakly affected by the growth conditions. In this case the volume ratio of the defective layer versus relatively defect-free core becomes very significant and thus contribution of the surface and near-surface states should in principle increase because of that.

Recently published reports (e.g., [27–34]) addressed the relationship between the size of the ZnO nanostructures and their visible defect emission. There is certain evidence of the visible luminescence scaling with the crystal size, although the nature of defects responsible for this is not identified. In our earlier works we studied hexagonal ZnO nanorods synthesized via a low-budget multiparameter-controlled growth, employing low temperature wet precipitation [34, 35]. This protocol was designed for a size- and shape-selective growth of ZnO nanorods. Such selectivity was crucial for addressing the question of how the nanogeometry is affecting the surface defect properties. Crystal size and morphology of ZnO nanorods were controlled by the growth time and the solvent composition: both the longitudinal and transverse average dimensions of the obtained hexagonal nanorods as well as their morphological anisotropy were increasing with the growth time and water content in the solvent. We observed a strong correlation between nanocrystals' size/morphology and their optoelectronic defect-related properties.

In order to better elucidate the influence of the surface-to-volume ratio on the luminescent properties in nanocrystalline systems, not only the pure size effects but also the effects of dimensionality have to be investigated. In this paper we address this question for quasi-fractal-dimensional nanonetworks of hydrozincite. Knowing such structure-property relationship is important since it is related to the control parameters of the preparation method of complex ZnO nanomorphologies. For example, preparation of nanoscale ZnO without the hydrozincite precursor results in hexagonal particles, whereas with the help of the quasi-fractal hydrozincite it is relatively easy to prepare ZnO with the same quasi-fractal shapes. The growth method used in this work, similar to that presented in [15], employs accurate morphology control of the prepared nanoscale hydrozincite, as a promising precursor for photovoltaic and photocatalytic applications. Here we tackle the questions of the correlation between the optoelectronic properties of the obtained nanosystem and the quasi-fractal dimensionality of the studied specimens. To the best of our knowledge there were no published reports on the luminescent properties of nanoscale quasi-fractal-dimensional hydrozincite.

2. Materials and Methods

A set of samples with variable dimensionalities was made as follows. The specimens were prepared from $Zn(NO_3)_2{\cdot}6H_2O$ (Aldrich) and urea (Aldrich) in Milli-Q water, with the initial concentrations of Zn^{2+} ions and urea of 0.01 M and 0.05 M, respectively. Fresh stock solutions were prepared to avoid hydrolysis upon storage. All reagents were of an analytical reagent grade. The sample growth was carried out in 600 mL closed glass reactor bottles, placed in an oven preheated at 90°C, with the total volume of reaction mixture of 425 mL. The temperature was measured in the center of the reactor by a Pt100 sensor. The maximum temperature, 84°C, was reached after around 120 minutes and was kept constant during the synthesis. Three different growth times, 2, 4, and 48 hours, were applied. The resulting solids were filtered off, washed with water, and dried in air.

Composition of the specimens was determined using the Fourier transform infrared (FTIR) spectroscopy. The IR spectra were obtained on an FTIR spectrometer (Perkin Elmer 2000) in the spectral range between 4000 and 400 cm^{-1} with a spectral resolution of 4 cm^{-1} in the transmittance mode. The KBr pellet technique was used for sample preparation.

Samples were also characterized by a field emission scanning electron microscope (SEM) Zeiss Supra 35 VP with an EDS analyzer.

We employed photoluminescence spectroscopy (PL) as a characterization probe of the optoelectronic properties of the studied specimens. The PL signal was excited by a CW Kimmon IK5452R-E HeCd laser with a wavelength of 325 nm. A variable frequency chopper was employed to provide a reference frequency. The samples were mounted inside an evacuated Janis CCS-150 cryostat having a temperature range between 8 and 325 K. The PL signal was probed by a Spex 1401 monochromator with a spectral resolution of 0.18 cm^{-1} and an RCA C31034 photomultiplier tube detector connected to a Stanford Research-830 lock-in amplifier for a background noise reduction.

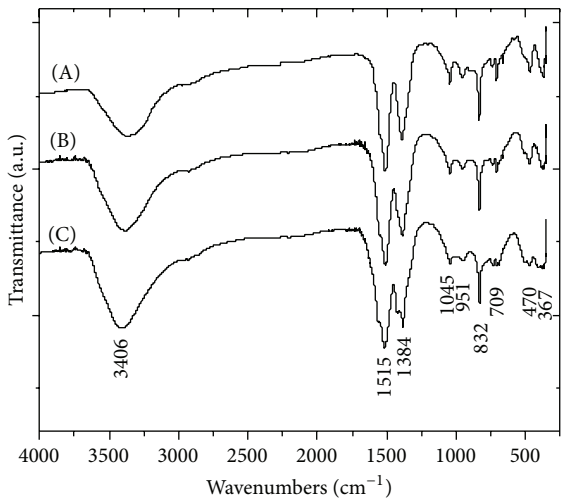

Figure 1: FTIR spectra of the samples prepared after 48 (A), 4 (B), and 2 (C) hours.

3. Results and Discussion

The FTIR spectra of the prepared samples are presented in Figure 1. The prevailing abundance of the carbonate groups from the precipitated $Zn_5(OH)_6(CO_3)_2$ in the final product is clearly confirmed by the bands in the 1600 and 600 cm^{-1} range in all samples. The bands for ZnO are expected in the range from 500 to 400 cm^{-1}. Since hydrozincite has its own bands in that region we could not exclude presence of the ZnO phase in the samples. The XRD spectra of similar samples were presented elsewhere [15], and the major peaks of these XRD spectra correspond to primarily $Zn_5(OH)_6(CO_3)_2$.

The SEM images of the obtained samples are shown in Figures 2–4. As one can see, the material grown for the longest (48 hrs) time interval exhibits a distinct 2D morphology. The morphology of the sample grown during the 2-hour period is quasi 1D, consisting of a network of nanowires, whereas the dimensionality of the 4-hour sample is of intermediate (1.xD) dimensionality. One can see that with the increase of the growth time the nanowires start to expand sideways and acquire first a leaf-like and then a platelet-like morphology. Notably, the characteristic scale of the obtained nanostructures does not change significantly with the growth time. Thus, our growth procedure provides consistent sampling of the hydrozincite nanostructures to address the effects of a quasi-fractal dimensionality and shape on the defect luminescence, where the growth time serves as a control parameter.

We ran room and low temperature PL experiments on these samples (Figures 5 and 6). The ubiquitous hydrozincite blue emission band can be observed at ~2.9 eV in all the spectra with approximately the same location independent of the temperature and morphology. On the other hand, in the spectra of the 2D and 1.xD samples one can also see a band at ~2.4 eV at both room and low temperatures. For the 1D sample, the blue ~2.9 eV luminescence band is accompanied by a broad spectral feature at ~2.2 eV for both figures. Finally,

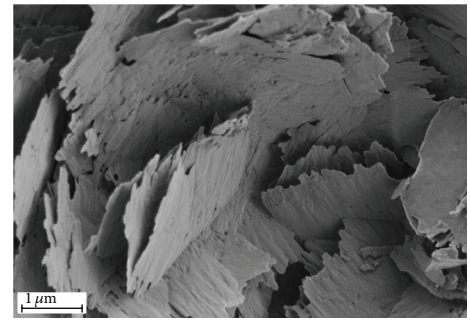

Figure 2: SEM image of the sample obtained after 48 hrs of synthesis.

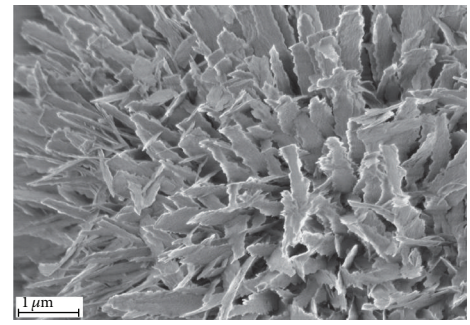

Figure 3: SEM image of the sample obtained after 4 hrs of synthesis.

at room temperature, in the higher-dimensional samples there is a single peak at ~3.3 eV, and at low temperature there is a series of relatively narrow peaks in the high-energy part of the spectrum. We submit that these features are consistent with common ZnO luminescence spectra, where the 2.2 eV and 2.4 eV features are the deep defect-related bands and the UV peaks are associated with the near-band edge (NBE) transitions, such as excitonic luminescence and its phonon replicas. Moreover, one can see a significant correlation between the sample dimensionality, on the one hand, and the relative intensity of the defect versus NBE emission ratio, on the other. For the room temperature PL, the relative intensity of the ZnO deep defect emissions and the blue hydrozincite luminescence grows with the decrease of the dimensionality, and the band gap luminescence disappears for the 1D sample. Similarly, for the 8 K PL spectra, the spectral features in the visible have a visibly higher intensity for the 1D structures compared to those of the 2D sample, while the NBE emissions observed in the 2D system are reduced by an order of magnitude in the 1D material.

The observed spectral behavior can be explained in terms of a likely coexistence of two phases, those of zinc oxide and hydrozincite, in the studied samples. Evidently, the relative abundance of ZnO is below the sensitivity levels of FTIR and XRD [12], whereas it is readily detectable by PL, because of the well-known exceptional luminescence characteristics of zinc oxide. The significant correlation between the quasi-fractal dimensionality of the samples and the ZnO- and $Zn_5(OH)_6(CO_3)_2$-related emissions could be indicative of an elevated defect contribution in crystals with smaller

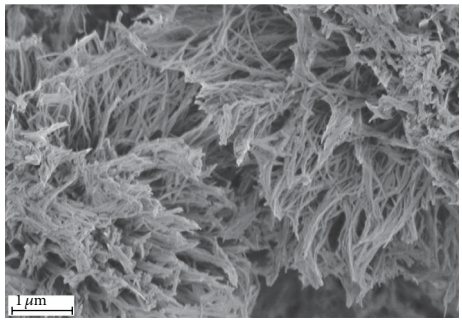

Figure 4: SEM image of the sample obtained after 2 hrs of synthesis.

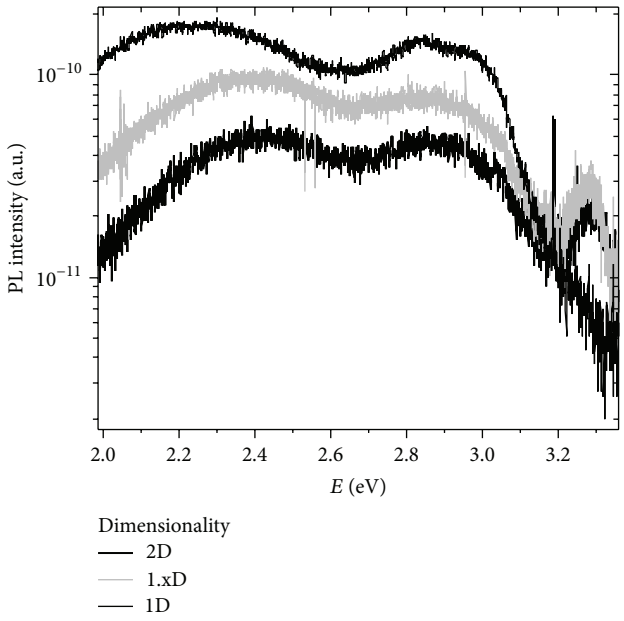

Figure 5: Comparison between room temperature PL spectra of the samples of variable dimensionality.

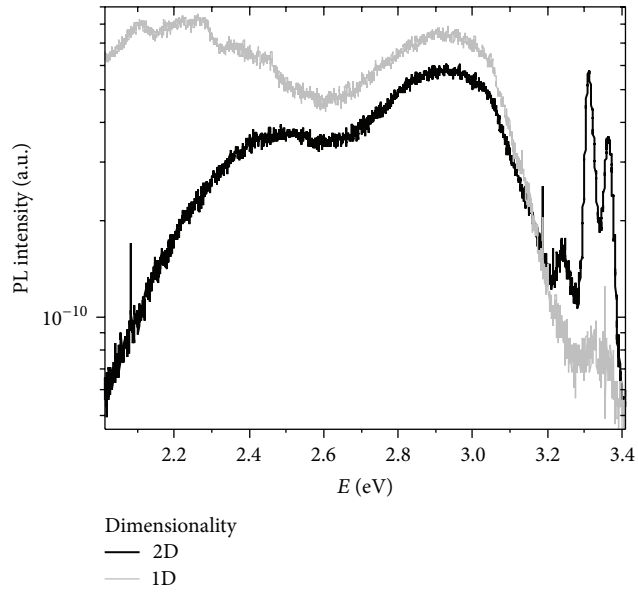

Figure 6: Comparison between low temperature (8 K) PL spectra of the samples of variable dimensionality.

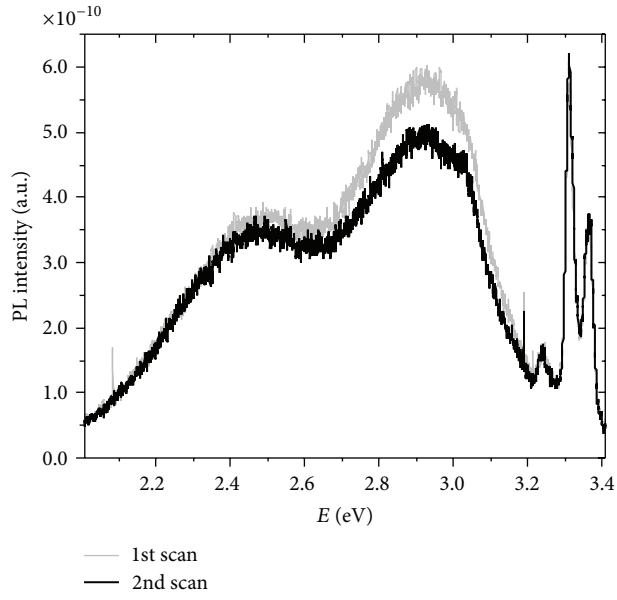

Figure 7: Comparison between low temperature (8 K) PL spectra of the 2D sample collected within a 1-hour interval during a continuous laser beam irradiation.

dimensionalities and, therefore, in a good agreement with the assumption that the surface and near-surface defect contribution increases with the decrease of the quasi-fractal dimensionality and hence the surface-to-volume ratio (a greater volume fraction of the defect-rich near-surface layers). The two-phase structure of the specimens is further confirmed by the dependence of the spectral shape on the time of exposure to the laser beam. Figure 7 illustrates a typical example of such dependence, where the two spectra of the 2D sample shown were collected at 8 K within a 1-hour interval of a continuous laser beam irradiation. One can see a relative constancy of the ZnO-related emission, whereas the intensity of the blue hydrozincite emission band is reduced by almost 20%. It is well known that annealing of nanoscale hydrozincite leads to its transformation into ZnO [10–17] so local heating produced by the laser beam may contribute to partial reduction of the relative abundance of the hydrozincite phase.

Time dependence shown in Figure 7 was observed consistently for all other samples (not shown). An additional corroboration for the presence of the ZnO phase in the material is a shift in the position of the deep defect band from 2.4 eV to 2.2 eV occurring at both temperatures with the decreasing dimensionality of the nanostructures. A very similar shift (2.4 eV to 2.2 eV) of the deep defect emission was observed in PL spectra of ZnO nanopowders with the decrease of an average grain size [36, 37]. It should be noted that an unambiguous assignment of the optical transitions to specific defects in ZnO is still under debate. Moreover, recent theoretical studies for single native defects offer plausible

explanation for such uncertainty in assignment, resulting from a multitude of possible transitions with similar energy differences involving different charge states of assorted native defects [38]. A similar statement can be applied to the blue hydrozincite luminescence. For example, it is unlikely that the lead impurity (cf. [23]) is the primary source of this emission band in the studied samples since our growth procedure did not employ any Pb content.

It should be noted that, in principle, different morphologies of the samples may affect scattering and/or absorption in PL experiment. However, this factor is not likely to be the main source of the spectral differences observed in our work. ZnO-related PL features similar to those reported here were observed by us in nanoscale ZnO specimens with completely different morphologies [34]. Moreover, time dependent spectra (cf. Figure 7) indicate that the observed spectral transformations result primarily from variance in composition and/or relative abundance of radiative centers.

4. Conclusions

PL experiments on the quasi-fractal-dimensional hydrozincite/zinc oxide nanonetworks revealed a strong correlation between the dimensionality/morphology of the nanocrystals and their defect optoelectronic properties, confirming hypothesis that the contribution of defects should increase with the increasing surface-to-volume ratio of the nanocrystal. Careful control of the quasi-fractal dimensionality of such nanonetworks and their surface properties can be vital for efficient operation of underlying photovoltaic devices. Furthermore, such elucidation of the structure-property relationship for the nanostructured precursor could be relied on for the proper choice of the processing parameters during its conversion into a final product, ZnO with a complex nanomorphology.

Conflict of Interests

The authors declare that there is no conflict of interests regarding the publication of this paper.

Acknowledgments

This work was in part supported by the TCU RCAF Grant no. 60535 (YMS) and the Slovenian Research Agency (Program P1-0030).

References

[1] Ü. Özgür, Y. I. Alivov, C. Liu et al., "A comprehensive review of ZnO materials and devices," *Journal of Applied Physics*, vol. 98, no. 4, Article ID 041301, pp. 1–103, 2005.

[2] Z. L. Wang, "Zinc oxide nanostructures: growth, properties and applications," *Journal of Physics Condensed Matter*, vol. 16, no. 25, pp. R829–R858, 2004.

[3] M. Bitenc and Z. C. Orel, "Hydrothermal growth of $Zn_5(OH)_6(CO3)_2$ and its thermal transformation into porous Zno film used for dye-sensitized solar cells," *Materiali in Tehnologije*, vol. 45, no. 3, pp. 287–292, 2011.

[4] S. Ueno and S. Fujihara, "Controlled synthesis of nanostructured ZnO films for use in dye-sensitized solar cells," *Journal of the Electrochemical Society*, vol. 158, no. 1, pp. K1–K5, 2011.

[5] N. C. Das, S. Biswas, and P. E. Sokol, "The photovoltaic performance of ZnO nanorods in bulk heterojunction solar cells," *Journal of Renewable and Sustainable Energy*, vol. 3, no. 3, Article ID 033105, 2011.

[6] C. K. Xu, K. K. Yang, L. W. Huang, and H. Wang, "Vertically aligned ZnO nanodisks and their uses in bulk heterojunction solar cells," *Journal of Renewable and Sustainable Energy*, vol. 2, no. 5, Article ID 053101, 2010.

[7] P. X. Gao, J. Song, J. Liu, and Z. L. Wang, "Nanowire piezoelectric nanogenerators on plastic substrates as flexible power sources for nanodevices," *Advanced Materials*, vol. 19, no. 1, pp. 67–72, 2007.

[8] H. Noh, M. Scharrer, M. A. Anderson, R. P. H. Chang, and H. Cao, "Photoluminescence modification by a high-order photonic band with abnormal dispersion in ZnO inverse opal," *Physical Review B: Condensed Matter and Materials Physics*, vol. 77, no. 11, Article ID 115136, 2008.

[9] Z. L. Wang, "Piezoelectric nanostructures: From growth phenomena to electric nanogenerators," *MRS Bulletin*, vol. 32, no. 2, pp. 109–116, 2007.

[10] M. Bitenc, P. Podbršček, P. Dubček et al., "In and Ex situ studies of the formation of layered microspherical hydrozincite as precursor for ZnO," *Chemistry A: European Journal*, vol. 16, no. 37, pp. 11481–11488, 2010.

[11] S. A. M. Lima, F. A. Sigoli, J. Jafelicci M., and M. R. Davolos, "Luminescent properties and lattice defects correlation on zinc oxide," *International Journal of Inorganic Materials*, vol. 3, no. 7, pp. 749–754, 2001.

[12] N. Kanari, D. Mishra, I. Gaballah, and B. Dupré, "Thermal decomposition of zinc carbonate hydroxide," *Thermochimica Acta*, vol. 410, no. 1-2, pp. 93–100, 2004.

[13] C. Yan and D. Xue, "Morphosynthesis of hierarchical hydrozincite with tunable surface architectures and hollow zinc oxide," *Journal of Physical Chemistry B*, vol. 110, no. 23, pp. 11076–11080, 2006.

[14] Y. Liu, Z. Jian-er, A. Larbot, and M. Persin, "Preparation and characterization of nano-zinc oxide," *Journal of Materials Processing Technology*, vol. 189, no. 1–3, pp. 379–383, 2007.

[15] M. Bitenc, M. Marinšek, and Z. C. Orel, "Preparation and characterization of zinc hydroxide carbonate and porous zinc oxide particles," *Journal of the European Ceramic Society*, vol. 28, no. 15, pp. 2915–2921, 2008.

[16] Z. Jing and J. Zhan, "Fabrication and gas-sensing properties of porous ZnO nanoplates," *Advanced Materials*, vol. 20, no. 23, pp. 4547–4551, 2008.

[17] R. Wahab, S. G. Ansari, Y. S. Kim, M. A. Dar, and H. S. Shin, "Synthesis and characterization of hydrozincite and its conversion into zinc oxide nanoparticles," *Journal of Alloys and Compounds*, vol. 461, no. 1-2, pp. 66–71, 2008.

[18] Y. Zheng, C. Chen, Y. Zhan et al., "Luminescence and photocatalytic activity of ZnO nanocrystals: correlation between structure and property," *Inorganic Chemistry*, vol. 46, no. 16, pp. 6675–6682, 2007.

[19] X. Dong, P. Yang, J. Wang, and B. Huang, "ZnO rhombic sheets of highly crystalline particles and their composite with Ag_2O toward efficient photocatalysis," *ChemPlusChem*, vol. 79, no. 12, pp. 1681–1690, 2014.

[20] P. B. Himelfarb, G. W. Simmons, K. Klier, and R. G. Herman, "Precursors of the copper-zinc oxide methanol synthesis catalysts," *Journal of Catalysis*, vol. 93, no. 2, pp. 442–450, 1985.

[21] P. Porta, S. de Rossi, G. Ferraris, M. lo Jacono, G. Minelli, and G. Moretti, "Structural characterization of malachite-like coprecipitated precursors of binary CuO-ZnO catalysts," *Journal of Catalysis*, vol. 109, no. 2, pp. 367–377, 1988.

[22] G. de Giudici, F. Podda, R. Sanna et al., "Structural properties of biologically controlled hydrozincite: an HRTEM and NMR spectroscopic study," *American Mineralogist*, vol. 94, no. 11-12, pp. 1698–1706, 2009.

[23] M. Gaft, R. Reisfeld, and G. Panczer, *Modern Luminescence Spectroscopy of Minerals and Materials*, Springer, Berlin, Germany, 2005.

[24] A. Kolodziejczak-Radzimska and T. Jesionowski, "Zinc oxide-from synthesis to application: a review," *Materials*, vol. 7, no. 4, pp. 2833–2881, 2014.

[25] F. A. Sigoli, M. R. Davolos, and M. Jafelicci Jr., "Morphological evolution of zinc oxide originating from zinc hydroxide carbonate," *Journal of Alloys and Compounds*, vol. 262-263, pp. 292–295, 1997.

[26] Z. Xingfu, H. Zhaolin, F. Yiqun, C. Su, D. Weiping, and X. Nanping, "Microspheric organization of multilayered ZnO nanosheets with hierarchically porous structures," *Journal of Physical Chemistry C*, vol. 112, no. 31, pp. 11722–11728, 2008.

[27] A. B. Djurišić and Y. H. Leung, "Optical properties of ZnO nanostructures," *Small*, vol. 2, no. 8-9, pp. 944–961, 2006.

[28] I. Shalish, H. Temkin, and V. Narayanamurti, "Size-dependent surface luminescence in ZnO nanowires," *Physical Review B—Condensed Matter and Materials Physics*, vol. 69, no. 24, 4 pages, 2004.

[29] A. van Dijken, E. A. Meulenkamp, D. Vanmaekelbergh, and A. Meijerink, "Luminescence of nanocrystalline ZnO particles: the mechanism of the ultraviolet and visible emission," *Journal of Luminescence*, vol. 87, pp. 454–456, 2000.

[30] A. van Dijken, J. Makkinje, and A. Meijerink, "The influence of particle size on the luminescence quantum efficiency of nanocrystalline ZnO particles," *Journal of Luminescence*, vol. 92, no. 4, pp. 323–328, 2001.

[31] M. H. Huang, Y. Wu, H. Feick, N. Tran, E. Weber, and P. Yang, "Catalytic growth of zinc oxide nanowires by vapor transport," *Advanced Materials*, vol. 13, no. 2, pp. 113–116, 2001.

[32] Y. Yang, B. K. Tay, X. W. Sun et al., "Quenching of surface-exciton emission from ZnO nanocombs by plasma immersion ion implantation," *Applied Physics Letters*, vol. 91, no. 7, Article ID 071921, 2007.

[33] Y. Yang, X. W. Sun, B. K. Tay, P. H. T. Cao, J. X. Wang, and X. H. Zhang, "Revealing the surface origin of green band emission from ZnO nanostructures by plasma immersion ion implantation induced quenching," *Journal of Applied Physics*, vol. 103, no. 6, Article ID 064307, 2008.

[34] M. Bitenc, P. Podbršček, Z. C. Orel et al., "Correlation between morphology and defect luminescence in precipitated ZnO nanorod powders," *Crystal Growth and Design*, vol. 9, no. 2, pp. 997–1001, 2009.

[35] M. Bitenc and Z. Crnjak Orel, "Synthesis and characterization of crystalline hexagonal bipods of zinc oxide," *Materials Research Bulletin*, vol. 44, no. 2, pp. 381–387, 2009.

[36] R. M. Peters, J. A. Paramo, C. A. Quarles, and Y. M. Strzhemechny, "Correlation between optoelectronic and positron lifetime properties in as-received and plasma-treated ZnO nanopowders," in *Proceedings of the 20th International Conference on the Application of Accelerators in Research and Industry (CAARI '08)*, F. D. McDaniel and B. L. Doyle, Eds., pp. 965–969, August 2008.

[37] J. A. Paramo, R. M. Peters, C. A. Quarles, H. Vallejo, and Y. M. Strzhemechny, "Defect properties of ZnO nanopowders and their modifications induced by remote plasma treatments," *IOP Conference Series: Materials Science and Engineering*, vol. 6, no. 1, Article ID 012030, 2009.

[38] P. Erhart, K. Albe, and A. Klein, "First-principles study of intrinsic point defects in ZnO: role of band structure, volume relaxation, and finite-size effects," *Physical Review B: Condensed Matter and Materials Physics*, vol. 73, no. 20, Article ID 205203, 2006.